$^{40}Ar/^{39}Ar$ and ESR/U-series dates for Guado San Nicola, Middle Pleistocene key site at the Lower/Middle Palaeolithic transition in Italy

Alison Pereira, Sébastien Nomade, Qingfeng Shao, Jean-Jacques Bahain, Marta Arzarello, Eric Douville, Christophe Falguères, Norbert Frank, Tristan Garcia, Giuseppe Lembo, et al.

$^{40}Ar/^{39}Ar$ and ESR/U-series dates for Guado San Nicola, Middle Pleistocene key site at the Lower/Middle Palaeolithic transition in Italy

Alison Pereira [a, b, c, d, *], Sébastien Nomade [b], Qingfeng Shao [a, e], Jean-Jacques Bahain [a], Marta Arzarello [c], Eric Douville [b], Christophe Falguères [a], Norbert Frank [b, g], Tristan Garcia [f], Giuseppe Lembo [c], Brunella Muttillo [c], Vincent Scao [b], Carlo Peretto [c]

[a] Département de Préhistoire du Muséum national d'Histoire naturelle, UMR 7194 du CNRS, 1 rue René Panhard, 75013, Paris, France
[b] Laboratoire des Sciences du Climat et de l'Environnement, LSCE/IPSL, CEA-CNRS-UVSQ, Université Paris-Saclay, F-91191, Gif-sur-Yvette, France
[c] Sezione di Scienze Preistoriche e Antropologiche, Dipartimento di Studi Umanistici, Università degli Studi di Ferrara, C.so Ercole d'Este I, 32, Ferrara, Italy
[d] Ecole française de Rome, Piaza Farnese, IT-00186, Roma, Italy
[e] College of Geographical Science, Nanjing Normal University, Nanjing, 210023, China
[f] CEA, LIST, Laboratoire National Henri Becquerel, 91191, Gif-sur-Yvette Cedex, France
[g] Institute of Environmental Physics, Heidelberg University, Germany

Abstract

The Middle Pleistocene archaeological site of Guado San Nicola was discovered in 2005 in a fossil fluvial terrace of the Volturno River, close to the village of Monteroduni, Molise, Italy. Palaeontological remains and lithic artefacts, including both handaxes and Levallois, discoid and opportunistic debitage, were recovered in fluvial and slope sediments rich in volcanoclastic materials. This site includes four distinct human occupation levels. In two of them both "shaping-façonnage" and "knapping-débitage" technologies are highlighted, placing this site at the Lower/Middle Palaeolithic transition.

In the present study, geochronological analyses by $^{40}Ar/^{39}Ar$ on single-crystal and ESR/U-series on teeth were performed to precise the chronological framework of the occupations. The $^{40}Ar/^{39}Ar$ data obtained securely bracket the human occupation levels at the transition between the interglacial and glacial marine isotopic stages MIS 11 (i.e. 400 ± 9 ka) and MIS 10 (i.e. 345 ± 9ka). The weighted mean age obtained from ESR/U-series dating of six teeth (i.e. 364 ± 36 ka) is in very good agreement with the $^{40}Ar/^{39}Ar$ results. The radio-isotopic constraints we presented place the Guado San Nicola site as one of the earliest testimonies of Levallois debitage in Western Europe and confirm the potential and accuracy of paleo-dosimetric methods to date Middle Pleistocene sites.

Keywords
$^{40}Ar/^{39}Ar$ dating, ESR/U-series, Italy, Middle Palaeolithic transition, Levallois technologies

1. Introduction

The Palaeolithic site of Guado San Nicola (GSN), located close to the village of Monteroduni in Molise region (Central Italy), is only 10 km south of the early Middle Pleistocene Isernia la Pineta archaeological site (Fig. 1) (Peretto et al., 2015a, Peretto et al., 2015b). It was discovered in 2005 and has been excavated between 2008 and 2012 by a team directed by Carlo Peretto from the Università degli Studi di Ferrara. An impressive amount of archaeological remains (more than 4000 lithic artefacts and 1500 faunal remains) was hence recovered (Muttillo et al., 2014).

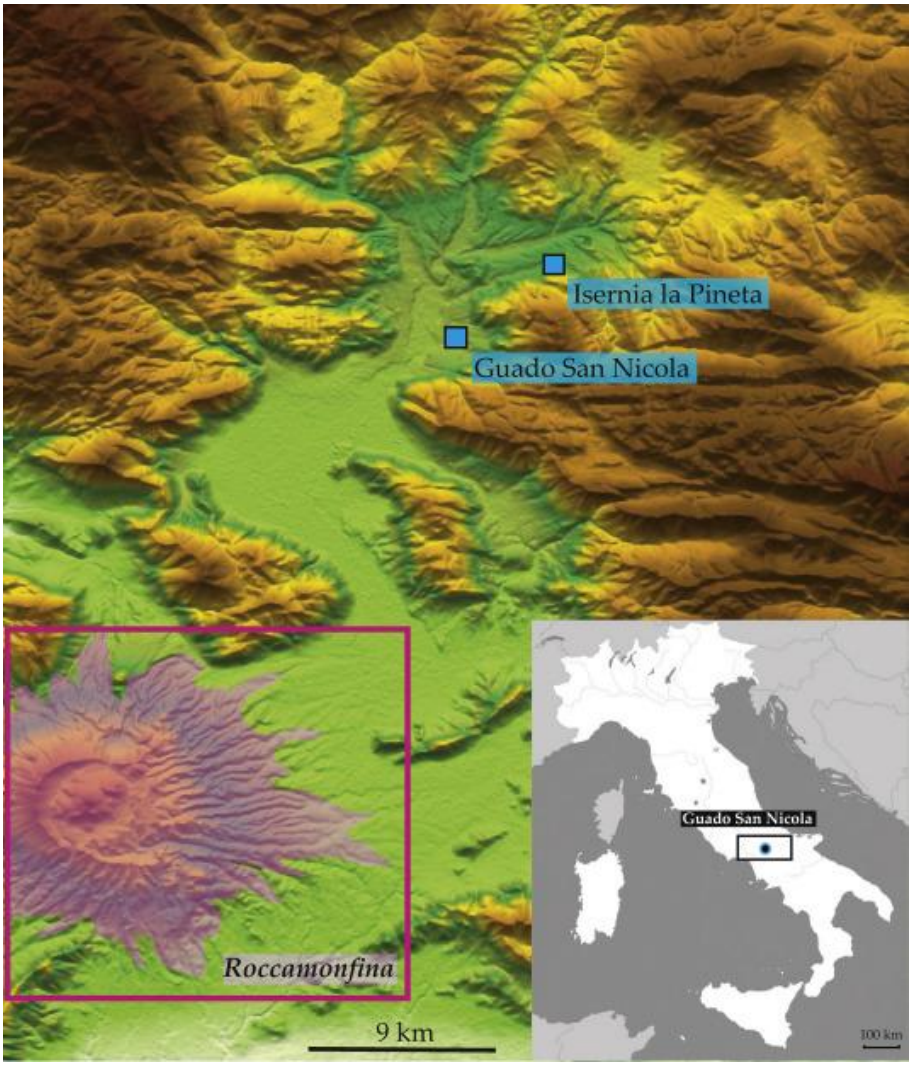

Fig. 1. Schematic geographical map of the Isernia basin, showing the Roccamonfina volcanic complex and the Guado San Nicola and Isernia la Pineta sites location.

The palaeontological assemblage is characteristic of the final Italian Galerian stage in Lazio. It is represented by a relative low species diversity, mainly dominated by the presence of cervids remains (*Cervus elaphus acoronatus*). This assemblage is commonly associated to woodland and bushes areas (Sala et al., 2014). The presence of *Equus ferus*, a large body size horse in this geographical area suggests that the palaeontological assemblage belongs probably to the recent part of the Fontana Ranuccio faunal unit (F.U.) (Masini and Sala, 2011), thus to the end of interglacial MIS 11 (Sala et al., 2014).

The lithic tools excavated present some singularities as the combination of Mode 2 and Mode 3 industries in almost all the archaeological levels within the sequence. The presence of numerous Levallois cores and flakes is significant (see details in Peretto et al., 2015b) and the use of this method increases upward along the stratigraphic sequence.

From technological viewpoint, Guado San Nicola is one of the rare Italian sites that present characteristic features of the Lower/Middle Palaeolithic transitional period (Muttillo et al., 2014). Dating the Guado San Nicola site is essential to better understand the geochronological context of this cultural transition in Italy. Hereafter, we present in detail the multi-methods approach we used to date this site. The Molise region was subjected to an intense volcanic activity during the Middle Pleistocene and thus several tephra layers are found in the archaeological sequences of the region (e.g.

Coltorti et al., 2005, Peretto et al., 2015a, Peretto et al., 2015b). At Guado San Nicola, archaeological layers directly include volcanic pumices and minerals. The site is capped by a direct tephra fallout (Fig. 2). The more proximal active volcano is the Roccamonfina complex located only 30 km South East of the site (Giannetti, 2001) (Fig. 1). This geological environment enables the use of the $^{40}Ar/^{39}Ar$ on single-crystal laser fusion dating method. As previously shown in Pereira et al. (2015) for the site of Notarchirico (Basilicata), this method is particularly pertinent to date archaeological sequences including both primary volcanic falls and reworked volcanic material deposits. Thanks to the richness of the palaeontological assemblage found at Guado San Nicola, it is also possible to apply the coupled ESR/U-series method through the analyses of large mammal tooth enamel. Results obtained following this double approach will be presented and discussed in detail hereafter.

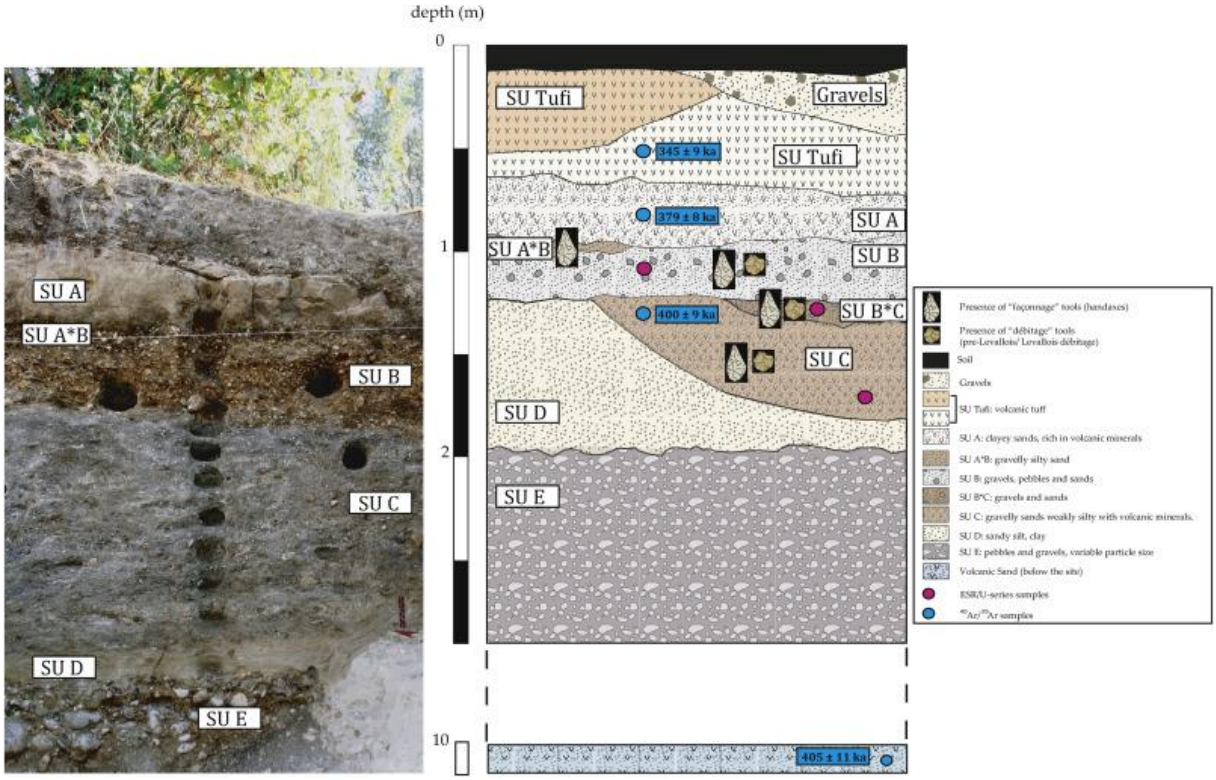

Fig. 2. Photo and schematic stratigraphy of Guado San Nicola showing the sampling positions for the $^{40}Ar/^{39}Ar$ and ESR/U-series methods and the archaeological deposits. The photo shows the excavation squares P11 and P12. S.U. Tufi is present on the first sector of the archaeological site not in the second one, that's why this layer isn't represented on the photo.

2. Geological setting

Guado San Nicola (250 m a.s.l) is located on the left bank of the Volturno River, in an ancient alluvial fan of the Lorda River, a tributary of the Volturno (Fig. 1). The Volturno valley is surrounded at the North by the Venafro and Mainarde mounts and at the South by the Matese Massif (Coltorti and Pieruccini, 2014). Geological and geomorphological analysis positioned Guado San Nicola within the oldest Middle Pleistocene Volturno fossil terrace identified in the valley (Coltorti and Cremaschi, 1981).

The stratigraphic sequence of the excavation site (2.5 m thick, Fig. 2), the palaeontological and lithic assemblages for the four identified archaeological levels (in stratigraphic unit (S.U.) C, S.U. B*C, S.U. B and S.U. A) are presented in detail in Turrini et al. (2014) and Peretto et al. (2015b) respectively. Fig. 2 summarises the different geological aspects of this sequence.

At the bottom, S.U. E (≈1.0 m thick layer), sterile from an archaeological viewpoint, is mainly composed of fluvial coarse gravels and sands (Turrini et al., 2014, Fig. 2). The overlying unit S.U. D is constituted by fluvial silts, sands and clays of typical floodplain environment. Its thickness varies on the excavated area from few centimetres to 15 cm (Fig. 2). The first sedimentary unit containing archaeological remains is S.U. C (variable thickness on the excavated area), it is composed of fluvial silts sands. This level includes also a high percentage of fresh volcanic pumices (Fig. 2). At its top, S.U. B*C (just recorded on a small area of the site, intercalated between S.U. C and S.U. B) presents a well-preserved archaeological palaeosurface overlying by the archaeological S.U. B unit (0–15 cm thick). S.U. B is mostly composed of sands and gravels with some volcanic elements and interpreted as the consequence of two successive local debris flows. It rests in erosive contact on S.U. C and B*C (Fig. 2). S.U. A*B above S.U. B is a thin layer (few centimetres) only recorded on a small area. This layer is made of alluvial deposits (with darker gravelly silty sands) influenced by pedogenetic phenomena. This unit contains both lithic industries and palaeontological remains (Fig. 2). S.U. A found on top of the two precedent units is a sandy slope deposit (earth flow) particularly rich in small pumices as well as clays and sterile from an archaeological perspective (Fig. 2).

Near the excavation area this layer is overlaid by S.U. Tufi, a primary volcanic fallout directly deposited in the Lorda River as highlighted by water circulation structures. The base of this unit (variable thickness) is white, while the superior part is darker, with a red colour, but its composition is homogeneous. Gravel slope deposits cutting S.U. Tufi and a pedological horizon end the sequence.

3. Sampling

Three samples for the $^{40}Ar/^{39}Ar$ dating were taken directly in the site in S.U. C, S.U. A and S.U. Tufi, respectively. S.U. Tufi corresponds to a direct volcanic fallout. The primary nature of the pumices found in S.U. C and S.U. A is questionable and more probably correspond to a local reworking soon after the deposition of this material according to the freshness and angular nature of this material.

An additional $^{40}Ar/^{39}Ar$ sample was taken from volcanic sands found in a drill core 8 m below S.U. E.

For ESR/U-series analyses, six teeth (horses and rhinoceros) were sampled from collections of S.U. B (3 teeth), B*C (1 tooth) and C (2 teeth). In situ gamma-ray measurements and sediment sampling were done for the dose rate determination.

4. Material and methods

4.1. 40Ar/39Ar

The four samples were firstly crushed and sieved and more than thirty transparent and non-altered sanidines crystals, ranging size between 500 μm and 1 mm were handpicked under a binocular. Selected crystals were next leached with a 7% HF acid solution to remove the possibly remaining groundmass. These potassium feldspars were then loaded in aluminium disks and irradiated in the β1 tube of the Osiris reactor, CEA Saclay (France). Three distinct irradiations were performed (IRR 57 and 66 (60 min) for both S.U. Tufi and Volcanic sand and IRR 34 (90 min) for S.U. A and S.U. C). After irradiations, samples were separately transferred in a copper sample holder and put into a double vacuum Cleartran window. Crystals were next individually fused by a 25 Watt Synrad CO_2 laser (using 10–15% of the nominal power). The extracted gases were purified by two GP 110 getters (ZrAl) and argon isotopes (^{36}Ar, ^{37}Ar, ^{38}Ar, ^{39}Ar, ^{40}Ar) were measured using a VG5400 mass spectrometer equipped with an electron multiplier Balzers 217 SEV SEN coupled to an ion counter (full analytical protocol detailed in Nomade et al. (2010)). Neutron J fluence for each sample was calculating using co-irradiated Alder Creek Sanidine (ACs-2) standard with an age of 1.194 Ma (Nomade et al., 2005) (IRR 34, $J = 0.0007580 \pm 0.0000015$; IRR 57; $J = 0.00042460 \pm 0.0000017$; IRR 66; $J = 0{,}00036890 \pm 0.00000369$) and the total decay constant of Steiger and Jäger (1977).

Recent revisions of the standard and/or decay constants suggest values of about ±1% than the one we used (Kuiper et al., 2008, Renne et al., 2011, Phillips and Matchan, 2013, Rivera et al., 2013). Nevertheless, the difference in the final age for Middle Pleistocene levels dated is negligible. These ages remain within the full-propagated uncertainties (i.e. ± *4 ka)*. Procedural blank measurements are performed after every three unknown samples. For typical 9 min static blank, typical backgrounds are about $2.0–3.0 \times 10^{-17}$ and 5.0 to 6.0×10^{-19} mol for ^{40}Ar and ^{36}Ar respectively. The precision and accuracy of the mass discrimination correction was monitored by weekly measurements of air argon of various beam sizes and was calculated relative to a $^{40}Ar/^{36}Ar$ ratio of 298.56 (Lee et al., 2006).

4.2. ESR/U-series

The teeth were analyzed according to the experimental protocol described in Bahain et al. (2012). After mechanic separation of the different dental tissues, the outer surfaces of enamel layers were cleaned using a dentist drill in order to eliminate the effect of external alpha radiations. The radionuclides (primarily ^{238}U, ^{226}Ra and ^{222}Rn) in the dental tissues (enamel, dentine and cementum) were measured by low background high purity γ-spectrometry. These tissues were then analyzed by U-series with an Inductively Coupled Plasma-Quadrupole Mass Spectrometry (ICP-QMS) according to the chemical protocol of Shao et al. (2011), in order to obtain the $^{234}U/^{238}U$ and $^{234}U/^{230}Th$ ratios necessary for the calculation of the U-uptake parameters (Table 1).

Sample	Layer	Dental tissue	U (ppm)	$^{230}Th/^{232}Th$	$^{234}U/^{238}U$	$^{230}Th/^{234}U$	Age (ka)
SN1001	B	cement	40.76 ± 0.09	184	1.319 ± 0.004	1.133 ± 0.008	>500
		dentine	103.67 ± 0.45	3600	1.253 ± 0.003	0.950 ± 0.011	251 ± 12
		enamel	2.45 ± 0.01	42	1.303 ± 0.004	0.897 ± 0.011	207 ± 8
SN1002	B	cement	108.95 ± 0.44	574	1.234 ± 0.004	0.840 ± 0.007	180 ± 5
		dentine	121.74 ± 0.45	1512	1.248 ± 0.004	0.831 ± 0.009	175 ± 6
		enamel	2.96 ± 0.01	73	1.281 ± 0.004	0.765 ± 0.008	145 ± 4
SN0902	B	cement	38.99 ± 0.11	52	1.319 ± 0.003	1.167 ± 0.007	>500
		dentine	140.33 ± 0.43	4693	1.204 ± 0.003	0.855 ± 0.005	190 ± 4
		enamel	3.38 ± 0.01	100	1.223 ± 0.005	0.786 ± 0.005	155 ± 3
SN0906	B	dentine	67.27 ± 0.27	284	1.338 ± 0.006	1.048 ± 0.010	365 ± 31
		enamel	1.35 ± 0.01	7	1.254 ± 0.006	1.114 ± 0.010	>500
SN1003	B*C	dentine	86.26 ± 0.21	504	1.328 ± 0.004	1.055 ± 0.009	384 ± 31
		enamel	0.50 ± 0.01	3	1.230 ± 0.006	0.934 ± 0.012	241 ± 14
SN1004	C	dentine	83.68 ± 0.38	930	1.318 ± 0.003	1.051 ± 0.010	379 ± 29
		enamel	0.71 ± 0.01	16	1.402 ± 0.005	0.918 ± 0.011	213 ± 9

Table 1. U-series data obtained by Q-ICP-MS on dental tissues of analysed teeth from Guado San Nicola site. Analytical uncertainties are given at 2σ confidence.

The combination of γ-ray spectrometry and ICP-QMS analyzes also allows the estimation of eventual radium and radon losses (Bahain et al., 1992) (Table 2). Removed enamel thicknesses during the preparation process are also indicated Table 2 and used to correct for both internal and external β dose-rates (Brennan et al., 1997) (Table 2). The radionuclides in associated sediments recovered near the teeth were also measured by γ-spectrometry (Table 3) and in situ gamma measurements were also performed for each studied level in the sections located at the vicinity of the teeth discovery places when it was possible (see Supplementary Fig. S1). Water contents of the sediments were measured after one week drying in an oven at 40 °C. The mean value of 15 ± 5 wt % was used for all calculations. Water contents of 0 and 7 ± 5 wt% were used for enamel and dentine respectively (assumed values).

Sample	Layer	Dental tissue	$^{222}Rn/^{230}Th$	Initial enamel thickness (µm)	Removed enamel thickness – dentine side (µm)	Removed enamel thickness – cement or sediment side (µm)
SN1001	B	cement	0.290	1053 ± 132	68 ± 8	12 ± 1
		dentine	0.407			
		enamel	0.796			
SN1002	B	cement	0.352	1204 ± 151	67 ± 8	13 ± 2
		dentine	0.352			
		enamel	0.705			
SN0902	B	cement	0.307	1273 ± 159	32 ± 4	80 ± 10
		dentine	0.419			
		enamel	0.662			
SN1003	B*C	dentine	0.085	1793 ± 224	48 ± 6	58 ± 7
		enamel	0.779			
SN1004	C	dentine	0.363	2328 ± 291	56 ± 7	28 ± 4
		enamel	0.790			
SN0906	B	dentine	0.411	96 ± 237	67 ± 8	40 ± 5
		enamel	0.644			

Table 2. $^{226}Ra/^{230}Th$ et $^{222}Rn/^{230}Th$ isotopic coefficients and enamel preparation data measured on dental tissues of analysed teeth from Guado San Nicola site. Analytical uncertainties are given at 1σ confidence.

Sample	Layer	^{238}U (ppm)	^{232}Th (ppm)	^{40}K (%)
SN1001	B	4.20 ± 0.21	22.24 ± 0.35	3.68 ± 0.06
SN1002	B	3.73 ± 0.20	18.57 ± 0.34	4.06 ± 0.04
SN0902	B	5.24 ± 0.24	8.90 ± 0.11	3.68 ± 0.06
SN0906	B	3.71 ± 0.11	19.05 ± 0.33	3.64 ± 0.04
SN1003	B*C	3.40 ± 0.28	42.03 ± 0.57	2.95 ± 0.05
SN1004	C	4.51 ± 0.18	20.74 ± 0.29	6.21 ± 0.04

Table 3. Radionuclides contents of sediments from Guado San Nicola site measured by laboratory gamma-ray spectrometry. Analytical uncertainties are given at 1σ confidence.

The 100–200 µm grain-size fraction of enamel has been separated into ten aliquots. Nine of these were irradiated at the laboratory National Henri Becquerel of CEA (Saclay DEN) using a ^{60}Co gamma source at increasing doses (500, 800, 1,250, 2,000, 3,200, 5,000, 8,000, 12,500 and 20,000 Gy). ESR measurements (at least three measurements for each dose on different days) were performed on EMX Bruker ESR spectrometer at MNHN, Paris, using the following parameters: 10 mW microwave power, 0.1 mT modulation (100 kHz frequency modulation), room temperature, 10 mT scan range and 4 min scan time. The ESR intensities (I) of enamel aliquots were then measured from T1 to B2 peaks according to Grün (2000) in order to estimate the equivalent doses corresponding to the total doses of radiation received by the sample during its geological history. An "exponential plus linear" fitting function (E + L) (Berger and Huntley, 1989) was used for equivalent dose extrapolations performed on Microcal Origin Pro 8.0 with data weighting by $1/I^2$ (Grün and Brumby, 1994) (Supplementary Fig. S2).

Lastly, equivalent doses, ESR/U-series ages, different dose-rate contributions and U-uptake parameters were calculated using, according to the data, either US model (Grün et al., 1988) or AU model (Shao et al., 2012).

5. Results

5.1. $^{40}Ar/^{39}Ar$

Analytical details for each measured crystal are reported in the supplementary dataset (Tables S1–S4). Results are presented as probability diagrams Fig. 3 (Deino and Potts, 1990). When the geological deposit corresponds to a primary volcanic deposit (tephra), the age obtained gives directly the age of the eruption (i.e. deposition). When the deposit is composed of reworked volcanic material, the youngest sanidines population in the related probability diagram corresponds to the last volcanic eruption recorded in this layer and is interpreted as a minimum deposition age. Weighted mean ages and uncertainties are calculated using IsoPlot 3.0 (Ludwig, 2001) and given at 95% of probability, including the decay constant and the J flux. We include these uncertainties because we will compare results obtained by different geochronological methods (Renne et al., 2009). To be relevant, a homogeneous crystal population should present a Probability fit (P) > 0.1.

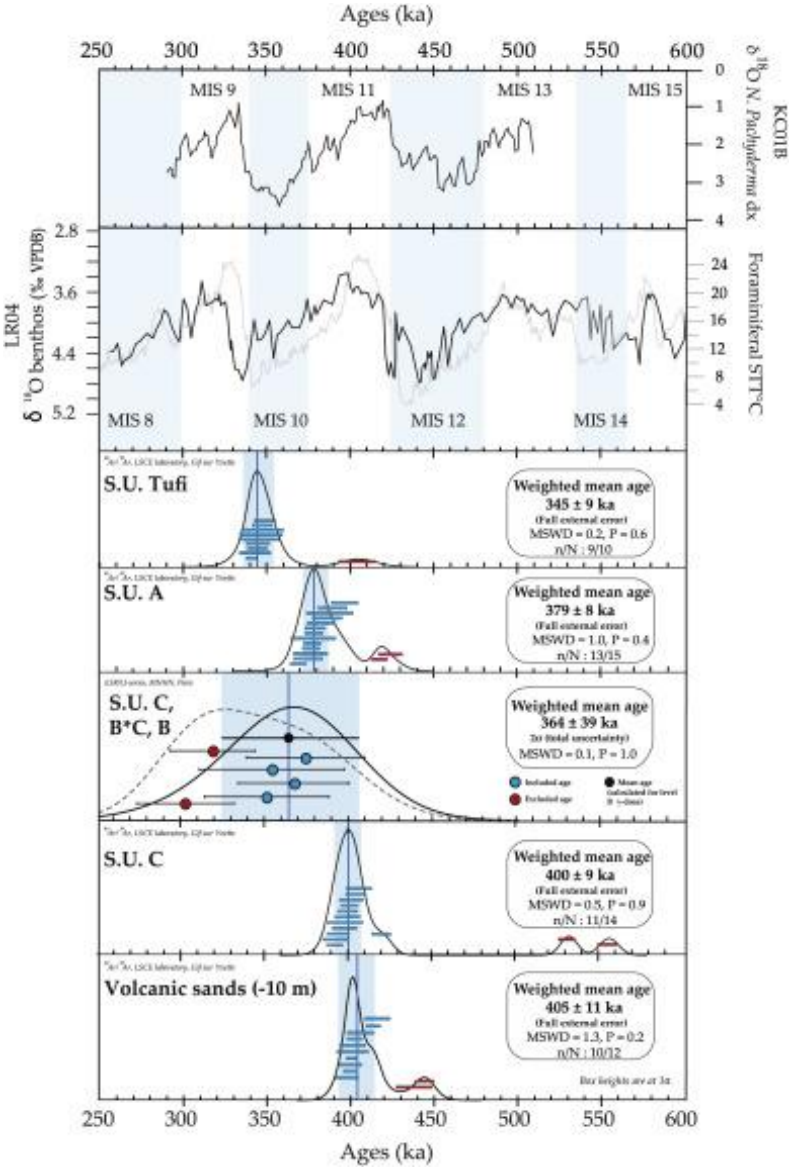

Fig. 3. $^{40}Ar/^{39}Ar$ results presented as probability diagrams and ESR/U-series ages calculated for S.U. B gamma dose-rate. Dotted curve for the ESR/U-series results demonstrates the weighted mean age for the six teeth measured. Ages are put in correlation with the LR04, $\delta^{18}O$ benthic curve (Lisiecki and Raymo, 2005) and with the ODP 975 Foraminiferal SST°C curve (Girone et al., 2013) and KC01b $\delta^{18}O$ planctonic curve (Capontondi et al., 2016).

5.1.1. Volcanic sand under S.U. E (−10 m)

A total of twelve sanidines were dated for this layer. The probability diagram displayed two modes (Fig. 3) corresponding to two volcanic eruptions recorded. The youngest population composed of ten crystals gives a weighted mean age of 405 ± 11 ka (95% confidence, P = 0.2). Corresponding inverse isochron initial $^{40}Ar/^{36}Ar$ ratio is imprecise because of the low spread but equivalent within uncertainty to the atmospheric ratio within uncertainties (see supplementary dataset Table S1).

5.1.2. S.U. C

Fourteen crystals were measured for S.U. C. The probability diagram obtained is bimodal with a homogeneous youngest crystals population. Only three grains are older than this population. The weighted mean age shows by this diagram for this main eruption is 400 ± 9 ka (P = 0.9). The inverse isochron initial $^{40}Ar/^{36}Ar$ ratio is equivalent to the atmospheric ratio within uncertainties (see supplementary dataset, Table S2). No excess argon has been detected.

5.1.3. S.U. A

Concerning S.U. A, fifteen crystals were analyzed. The probability diagram is really similar to the S.U. C one. The youngest population is homogeneous and only two grains belonged to older volcanic eruptions. The weighted mean age obtained for the youngest sanidines population is 379 ± 8 ka, (P = 0.4). The inverse isochron initial $^{40}Ar/^{36}Ar$ ratio is equivalent to the atmospheric ratio within uncertainties (see supplementary dataset, Table S3) and confirms the absence of excess argon inside the crystals.

The inverse isochron for both deposits present similar results as the probability diagrams.

5.1.4. S.U. Tufi

Ten grains were dated for S.U. Tufi tephra layer. The probability diagram is simple with one main mode. Only one crystal dated at 405 ka was found. The weighted mean age obtained for the primary population is 345 ± 9 ka (P = 1.0). The initial $^{40}Ar/^{36}Ar$ ratio given by the inverse isochron is 298.6 ± 4.0 ka identical to the atmospheric ratio, suggesting no argon excess in the crystals (see supplementary dataset, Table S4).

5.2. ESR/U-series

ESR/U-series age estimates and associated data obtained for the six Guado San Nicola teeth are displayed in Table 4.

Sample	Layer	Dental tissue	Equivalent dose (Gy)	U-Uptake parameter *p (US)* or n (AU)	Internal dose rate [a] (µGy/an)	External D_β dose rate (µGy/an)	D (γ+cosm) dose rate [b] (µGy/an)	Total dose-rate D_a (µGy/an)
SN1001	B	cementum	1029.35 ± 31.44	−0.00510 ± 0.00049	643 ± 154	1211 ± 211	1560 ± 150	3408 ± 301
		dentine		−0.00420 ± 0.00049				
		enamel		−0.00380 ± 0.00050				
SN1002	*B*	*cementum*	*1153.07 ± 19.57*	*−0.5487 ± 0.1060*	*584 ± 233*	*1170 ± 329*	*1560 ± 150*	*3304 ± 430*
		dentine		*−0.5177 ± 0.1107*				
		enamel		*−0.2504 ± 0.1504*				
SN0902	B	cementum	1192.69 ± 44.49	−0.00380 ± 0.00004	605 ± 160	1072 ± 223	1560 ± 150	3237 ± 313
		dentine		−0.00250 ± 0.00003				
		enamel		−0.00150 ± 0.00005				
SN0906	C	dentine	814.65 ± 25.81	−0.00420 ± 0.00004	438 ± 122	563 ± 96	1560 ± 150	2554 ± 216
		enamel		−0.00440 ± 0.00004				
SN1003	B*C	dentine	697.74 ± 73.77	−0.00450 ± 0.00067	135 ± 313	287 ± 149	1873 ± 95	2295 ± 359
		enamel		−0.00410 ± 0.00068				
		dentine		−0.00370 ± 0.00007	128 ± 272	283 ± 126	1560 ± 150	1971 ± 335
		enamel		−0.00330 ± 0.00007				
SN1004	C	dentine	886.84 ± 45.25	−0.00490 ± 0.00048	213 ± 134	628 ± 217	2260 ± 130	3101 ± 286
		enamel		−0.00420 ± 0.00049				
		dentine		−0.00350 ± 0.00044	204 ± 107	605 ± 172	1560 ± 150	2365 ± 227

		enamel		−0.00280 ± 0.00042				

Italics correspond to data not used for the final calculation.

[a] k-values of 0.13 ± 0.02 was used according with Grün and Katzenberger-Appel (1994).

[b] The cosmic dose rate was estimated from discovery depth using the formulae from Prescott and Hutton (1994).

Table 4. Equivalent doses, U-uptake parameters, different dose-rate contributions and ESR/U-series ages obtained on dental tissues of analyzed teeth from Guado San Nicola site. Analytical uncertainties are given with ± 2σ. For samples SN1003 and SN10004 the highlighted results are calculated using level B γ−dosimetry.

The US model has been applicable only to SN1002 tooth (S.U. B), all the other teeth display U-leaching evidence, increasing with depth. Indeed, we can notice that the ESR/U-series ages decrease as a function of depth while external doses increase In the same time, closed system U-series ages (Table 1), calculated taking into account an early uranium uptake assumption, increase and uranium contents decrease.

We interpreted that as an indication of a change in the dosimetric context of the lower geological units, in relation with water circulation during the implementation of the S.U. B slope deposit. This hypothesis is supported by the fact that the average in situ gamma dose-rate measured for S.U. B (1560 ± 150 μGy/a) provides the best isochronous results for the whole set of data (see Supplementary Fig. S3).

ESR/U-series ages were therefore calculated for the S.U. B*C and S.U. C samples using the S.U. B gamma dose-rate. The obtained ages range from 302 ± 25 ka (tooth SN1001, unit B) to 373 ± 35 ka (SN1004, unit C). Two ESR/U-series ages seems out of the $^{40}Ar/^{39}Ar$ dates range (SN1001, 302 ± 25 ka; SN0906, 319 ± 25 ka). Despite the stigmata of poor samples preservation and considering the four remaining samples ages, a mean age of 364 ± 39 ka (95% confidence, P = 1.0) representing the best ESR/U-series estimation for the S.U. B implementation can be obtained.

6. Discussion

6.1. Chronological framework for Guado San Nicola

The $^{40}Ar/^{39}Ar$ results demonstrate that the sediments found in the Guado San Nicola sequence site were deposited before 345 ± 9 ka, which corresponds to the weighted mean age obtained for the primary volcanic deposit S.U. Tufi (Fig. 3). All the $^{40}Ar/^{39}Ar$ ages are furthermore coherent from a stratigraphic viewpoint. They confirm the absence of important sedimentary reworking. The youngest populations of sanidines found in the volcanic sand below S.U. E (−10 m) and in S.U. C rework volcanic eruptions occurred during the full interglacial MIS 11 (405 ± 11 ka and 400 ± 9 ka respectively). The S.U. A displays a different source for the reworked volcanoclastic material. Thirteen on fifteen crystals dated are younger than the previous two units with a prominent population of crystals centred on 379 ± 9 ka suggesting that this unit was deposited between this age and 345 ± 9 ka (age for S.U. Tufi).

As the consequence of these results, all the archaeological levels (S.U. A*B, B, B*C and C) can be placed with confidence in the time range comprised between 400 ± 9 ka and 345 ± 9 ka at the transition between the isotopic marine stages MIS 11 and 10 (Fig. 3).

The analysis made by ESR/U-series method on teeth from different levels (S.U. B, B*C and C) allowed to calculate a statistically weighted mean age of 364 ± 39 ka. We interpreted this age as a minimum age for the deposition of the S.U. Bas we cannot determine precisely the onset time of the uranium uptake in the teeth because of frequent U-leaching evidence. This minimum age is in agreement within uncertainty with the bracket proposed based on the $^{40}Ar/^{39}Ar$ method.

6.2. Origin of the dated volcanic materials

The question of the origin of the volcanic material found at Guado San Nicola is essential and its answer could be found in the nearby volcanoes eruptive history. The size of the crystals analyzed (500 μm up to 1 mm) suggests a proximal eruptive source. The Roccamonfina stratovolcano located only 30 km South West of Guado San Nicola locality was really active during the MIS 11-10 period (Giannetti, 2001, Rouchon et al., 2008) (Fig 1). It represents the main potential source for the sanidines that we dated. The Colli Albani volcano, another potential volcanic source for this timescale, seems located too far (≈120 km northwest).

The Roccamonfina complex was in activity for the whole Middle Pleistocene period, between 550 and 95 ka and its tephrostratigraphy is today relatively well known (Giannetti, 2001, Rouchon et al., 2008). The formation and development of this stratovolcano was long and complex, but can be summarized in two main phases: A) a leucite-bearing stage (HKS) or Stage I from 550 to 375 ka, corresponding to the building of the main volcanic cone; B) a leucite-free low-K stage (LKS) or Stage II from 317 to 96 ka, marked by parasitic vents formation. An intermediate phase where both HKS and LKS volcanisms occurred is dated between 375 and 323 ka (Giannetti and De Casa, 2000, Giannetti, 2001). This period is characterized by a major ignimbrite forming eruption (named *Brown Leucitic Tuff*, BLT hereafter) responsible of the collapse of the central and northern part of the volcano (Luhr and Giannetti, 1987).

This eruptive period is partly coeval with the Guado San Nicola sequence deposition (c.a. 410 and 345 ka) and two eruptions dated to 403 ± 18 ka (c.a. Monte Ophelio, Rouchon et al., 2008) and 402 ± 18 ka at 2σ analytical respectively (Giannetti, 2001) could correspond to volcanic event evidenced in S.U. C and underlying sands. The ages of 379 ± 9 ka and 345 ± 9 ka found for S.U. A and the S.U. Tufi tephra respectively, are close in age with large ignimbritic eruptions from the intermediate phase where both HKS and LKS volcanisms occurred (Giannetti, 2001, Rouchon et al., 2008). Noticeably, the S.U. Tufi contains light brown pumices with altered leucites, dated in the present work to 345 ± 9 ka and could be correlated to the eruption found on the Devil's footsteps archaeological site, securely dated by $^{40}Ar/^{39}Ar$ at 345 ± 12 ka (2σ analytical) by Scaillet et al. (2008). This particular eruption is correlated by Scaillet and collaborators to the *Brown Leucitic Tuff* period. Additional $^{87}Sr/^{86}Sr$ analyses on clinopyroxenes from the different units are planned. They will allow to further characterize the geochemical signature of the reworked volcanic materials in the Guado San Nicola sequence.

6.3. Biostratigraphical age of the archaeological deposits

The palaeontological assemblage of Guado San Nicola is composed by *Ursus* sp., *Paleoloxodon* sp., *Stephanorhinus kirchbergensis*, *Equus ferus*, Megacerini, *Cervus elaphus acoronatus*, *Dama* sp. and *Bos primigenius*. It is a typical assemblage of the Middle Pleistocene "interglacial period", including both Galerian and Aurelian species associable to the Fontana Ranuccio FU biozone (Masini and Sala, 2011). The occurrence of *Cervus elaphus acoronatus* and *Equus ferus* support an age of occupation at the end of MIS 11. These observations are in agreement with the $^{40}Ar/^{39}Ar$ and ESR/U-series ages. Because of the interglacial characteristics of the palaeontological assemblage and according with the available geochronological data, we suggest that the human occupation levels of Guado San Nicola are bracketed between 400 and around 365 ka, predating the MIS 10 glacial stage (Fig. 4).

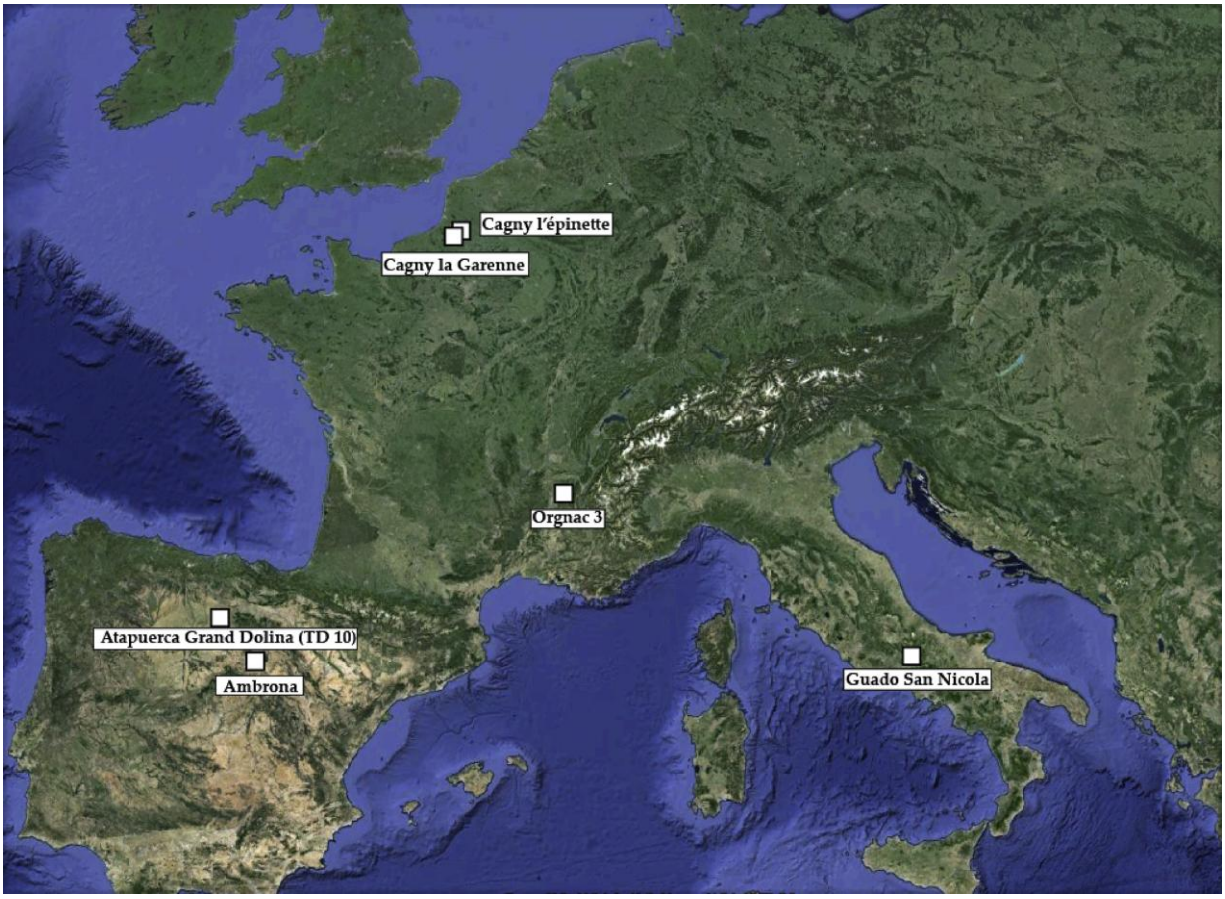

Fig. 4. Location of the archaeological sites of Cagny la Garenne, Cagny l'Epinette, Atapuerca Grand Dolina, Orgnac 3, Guado San Nicola and Ambrona.

6.4. Guado San Nicola in the Lower/Middle Palaeolithic transition context

According to our results, Guado San Nicola site should now be considered as the most ancient site in Italy and one of the most ancient in Europe that highlights the presence of Levallois method and its increasing mastery, combined to handaxes technologies (Peretto et al., 2015a, Peretto et al., 2015b). Our results strengthen the recent hypothesis that suggests a sporadic and asynchronous appearance in Europe of the Levallois technology with local technological development as early as MIS 11/MIS 10 without continuous geographical dispersion (Adler et al., 2014, Peretto et al., 2015a, Peretto et al., 2015b).

This transition however, currently corresponds to a large period of time mainly based on technical behaviours' changes as well as hominid anatomical evolutions during the late Middle Pleistocene. In Europe, this limit is generally associated to the progressive replacement of technological Mode 2 to Mode 3 (Clark, 1969) and by the Levallois technology generalization. Because of the several features and characteristics that encompassed the Lower/Middle Palaeolithic transition a strict temporal limit is probably impossible to draw. Indeed this transition does not appear to be linear and its timing seems to vary from one region to another (Terradillos-Bernal and Díez-Fernández-Lomana, 2012, Peretto et al., 2014, Peretto et al., 2015b). Finally, we must emphasize that according to the current knowledge and chronological constraints available for the Mode 2 and Mode 3, linked to Acheulean tools and Middle Palaeolithic technical cultures respectively, have coexisted for a long period of time in Europe (i.e 200 ka). Supporting a unique and universal boundary for this transition is thus particularly hazardous (Terradillos-Bernal and Díez-Fernández-Lomana, 2012).

The first occurrence of the Levallois débitage in Europe was dated around 450 ka at Cagny la Garenne I (France, Tuffreau et al., 2008) (Fig. 4). It corresponds chronologically to the transition between MIS

13 and MIS 12 (Tuffreau et al., 2008). In this site like at Guado San Nicola, bifacial industries were associated to Levallois débitage. In Southern Europe, the oldest occurrence of this technology was found at Atapuerca Gran Dolina TD 10 (Fig. 4) with a MIS 10 estimated age (Falguères et al., 2013, Moreno et al., 2015). During the MIS 9 and 8, more than a dozen of sites including Orgnac 3, Cagny l'Epinette, or Ambrona (located in Fig. 4) (Michel et al., 2013, Lamotte and Tuffreau, 2001, Falguères et al., 2006) displayed this technical behaviour. However, the "Levallois" generalization in Europe is much younger, between MIS 8 and 7 (Adler et al., 2014, Peretto et al., 2015a, Peretto et al., 2015b).

Other sites covering the MIS 11-9 period that show first Levallois development were dated by paleodosimetric methods (TL, OSL and ESR) or biochronology (Adler et al., 2014) and are not enough precisely dated to build a coherent catalogue of the "early" Levallois evolution in Western Europe. Guado San Nicola is the only site for this timescale in Europe on which radioisotopic, palaeodosimetric, palaeontological and archaeological data are in agreement, making this site one of the most significant for the understanding of the Middle Palaeolithic transition. Future investigations and new geochronological works when it is possible on the others are required to better understand the emergence of the Levallois technology between 400 and 300 ka.

7. Conclusion

The site of Guado San Nicola is now accurately dated to the end of MIS 11 by two different dating methods, a radioisotopic one ($^{40}Ar/^{39}Ar$) and a palaeodosimetric one (ESR/U-series). The new $^{40}Ar/^{39}Ar$ constraints allow the replacement of the Guado San Nicola human occupations between 400 ± 9 ka and 345 ± 9 ka (95% of probability). The ESR/U-series technic in agreement with the $^{40}Ar/^{39}Ar$ ages provided a deposition age of 364 ± 39 ka (95% of probability) for the stratigraphic level B. The presence of both Levallois, discoid and opportunistic methods and handaxes at Guado San Nicola makes of this settlement a key site in the debate around the understanding of the Lower/Middle Palaeolithic transition in Europe. Our results strengthen the hypothesis of an asynchronous appearance in Europe of the Levallois technology with local technological development starting as early as MIS 11/MIS 10.

The $^{40}Ar/^{39}Ar$ on single crystal method is one of the most accurate dating technic but is unfortunately not usable in all contexts as volcanic material is required. The absence of volcanic material in the most part of the European Middle-Pleistocene sites directly highlights the limit of the $^{40}Ar/^{39}Ar$ method in Europe. The $^{40}Ar/^{39}Ar$ results obtained at Guado San Nicola confirm that the ESR-U-series approach, despite a larger error range in comparison with isotopic geochronological methods, is available and useful to date Middle Pleistocene sites, if the U-uptake history of the samples is not too complex to reconstruct. We would like to emphasize that confront robust and precise methods such as $^{40}Ar/^{39}Ar$ or $^{230}Th/^{234}U$ with others methods usable in almost all archaeological sites the European (e.g. ESR/U-series on teeth, OSL, ESR on optically bleached quartz-) will allow to strengthen the confidence and comparison between ages obtained in various sites from the Lower-Middle Palaeolithic of Western Europe.

Acknowledgements

We would like to thank the Soprintendenza per i Beni Archeologici del Molise and the Direzione Regionale per i Beni Culturali e Paesaggistici del Molise for their collaboration. We thank also the "Ecole française de Rome" for financing A. Pereira's PhD project. In addition, the present study was financially supported by the ATM « Les dynamiques socio-ecosystémiques, entre perturbations et résiliences environnementales et culturelles » of the MNHN (project « Acheulean and volcanism in Italy » conducted by M.H. Moncel (MNHN) and J.J. Bahain (MNHN)) and the PHC Galileo project no. 28237WA 'l'Acheuléen en Italie méridionale: Chronologie, Paléoanthropologie, Cultures' led by J.J. Bahain (MNHN) and C. Peretto (Univ. of Ferrara) which allowed the funding of part of the field

missions. Finally, we particularly want to thank the two reviewers that help improved the overall quality of this manuscript.

References

D.S. Adler, K.N. Wilkinson, S. Blockley, D.F. Mark, R. Pinhasi, B.A. Schmidt-Magee, S. Nahapetyan, C. Mallol, F. Berna, P.J. Glauberman, Y. Raczynski-Henk, N. Wales, E. Frahm, O. Jöris, A. MacLeod, V.C. Smith, V.L. Cullen, B. Gasparian. **Early Levallois technology and the lower to Middle paleolithic transition in the Southern Caucasus.** Science, 345 (2014), pp. 1609-1613.

J.J. Bahain, C. Falguères, M. Laurent, Q. Shao, J.M. Dolo, T. Garcia, E. Douville, N. Frank, J.L. Monnier, B. Hallégouët, M. Laforge, B. Huet, P. Auguste, M. Liouville, F. Serre, J. Gagnepain Quat. Geochronol., 10 (July 2012), pp. 424-429.

J.J. Bahain, M.N. Sarcia, C. Falguères, Y. Yokoyama. **Attempt at ESR dating of tooth enamel of French middle Pleistocene sites.** Appl. Radiat. Isotopes., 44 (1-2) (1992), pp. 267-272.

G.W. Berger, D.J. Huntley. **Test data for exponential fits.** Anc. TL, 7 (1989), pp. 43-46

B.J. Brennan, W.J. Rink, E.L. McGuirl, H.P. Schwarcz, W.V. Prestwich. **Beta doses in tooth enamel by "One Group" theory and the Rosy ESR dating software.** Radiat. Meas., 27 (1997), pp. 307-314.

L. Capontondi, A. Girone, F. Lirer, C. Bergami, M. Verducci, M. Vallefuoco, A. Afferri, L. Ferraro, N. Pelosi, G.J. De Lange. **Central Mediterranean Mid-Pleistocene paleoclimatic variability and its association with global climate.** Palaeogeogr. Palaeoclimatol. Palaeoecol., 442 (2016), pp. 72-83.

G. Clark. **World Prehistory: A New Outline.** Cambridge University Press, London (1969), 284 pp.

M. Coltorti, M. Cremaschi. **Depositi quaternari e movimenti neotettonici nella conca di Isernia. Contributi conclusivi alla realizzazione della carta neotettonica d'Italia.** P.F.G., Sottoprogetto Neotettonica, CNR, Roma (1981), pp. 173-188.

M. Coltorti, G. Féraud, A. Marzoli, T. Ton-That, P. Voinchet, J.J. Bahain, A. Minelli, U. Thun Hoenstein. **New $^{40}Ar/^{39}Ar$, stratigraphic and palaeoclimatic data on the Isernia la Pineta Lower Palaeolithic site, Molise, Italy.** Quat. Int., 113 (2005), pp. 11-22.

M. Coltorti, P. Pieruccini. **Guado San Nicola Acheulean site: preliminary remarks on the litho-, morpho- and pedo-stratigraphical setting.** B. Muttillo, G. Lembo, C. Peretto (Eds.), L'insediamento a Bifacciali Di Guado San Nicola, Annali dell'Università degli Studi di Ferrara, Monteroduni, Molise, Italia (2014), pp. 13-24.

A. Deino, R. Potts. **Single-crystal $^{40}Ar/^{39}Ar$ dating of the olorgesailie formation, Southern Kenya Rift.** J. Geophys. Res., 95 (1990), pp. 8453-8470.

C. Falguères, J.J. Bahain, A. Pérez-González, N. Mercier, M. Santonja, J.M. Dolo. **The Lower Acheulian site of Ambrona, Soria (Spain): ages derived from a combined ESR/U- series model.** J. Archaeol. Sci., 33 (2006), pp. 149-157.

C. Falguères, J.J. Bahain, J.L. Bischoff, A. Pérez-González, A.I. Ortega, A. Ollé, A. Quiles, B. Ghaleb, D. Moreno, J.M. Dolo, Q. Shao, J. Vallverdú, E. Carbonell, J.M. Bermúdez de Castro, J.L. Arsuaga. **Combined ESR/U-series chronology of Acheulian hominid-bearing layers at Trinchera Galería site, Atapuerca (Spain).** J. Hum. Evol., 65 (2013), pp. 168-184.

B. Giannetti, G. De Casa. **Stratigraphy, chronology, and sedimentology of ignimbrites from the white trachytic tuff, Roccamonfina Volcano, Italy.** J. Volcanol. Geotherm. Res., 96 (2000), pp. 243-295.

B. Giannetti. **Origin of the calderas and evolution of the Roccamonfina volcano (Roman region, Italy).** J. Volcanol. Geotherm. Res., 106 (2001), pp. 301-319.

A. Girone, P. Maiorano, M. Marino, M. Kucera. **Calcareous plankton response to orbital and millennial-scale climate changes across the Middle Pleistocene in the western Mediterranean. Palaeogeography, Palaeoclimatology.** Palaeoecology, 392 (2013), pp. 105-116.

R. Grün. **Methods of dose determination using ESR spectra of tooth enamel.** Radiat. Meas., 32 (2000), pp. 767-772.

R. Grün, H.P. Schwarcz, J.M. Chadam. **ESR dating of tooth enamel: coupled correction for U-uptake and U-series disequilibrium.** Nucl. Tracks Radiat. Meas., 14 (1988), pp. 237-241.

R. Grün, S. Brumby. **The assessment of errors in past radiation doses extrapolated from ESR/TL dose-response data.** Radiat. Meas., 23 (1994), pp. 307-315.

R. Grün, O. Katzenberger-Appel. **An alpha irradiator for ESR dating.** Anc. TL, 12 (1994), pp. 35-38.

K.F. Kuiper, A. Deino, F.J. Hilgen, W. Krijgsman, P.R. Renne, J.R. Wijbrans. **Synchronizing rock clocks of Earth history.** Science, 320 (2008), pp. 500-504.

A. Lamotte, A. Tuffreau. A. Tuffreau (Ed.), L'Acheuléen dans la vallée de la Somme et Paléolithique moyen dans le nord de la France: données récentes, Centre d'Etudes et Recherches Préhistoriques, Lille, France (2001), pp. 149-153.

J.Y. Lee, K. Marti, J.P. Severinghaus, K. Kawamura, Y. Hee-Soo, J.B. Lee, J.S. Kim. **A redetermination of the isotopic abundances of atmospheric Ar.** Geochim. Cosmochim. Acta, 70 (2006), pp. 4507-4512, 10.1016/j.gca.2006.06.1563.

L.E. Lisiecki, M.E. Raymo. **A Pliocene-Pleistocene stack of 57 globally distributed benthic $d^{18}O$ records.** Paleoceanography, 20 (2005), p. PA1003, 10.1029/2004PA001071.

K.R. Ludwig. **Isoplot 3.0a geochronological toolkit for microsoft excel.** Special Publication No. 4, Berkeley Geochronology Center, Berkeley, CA (2001).

J.F. Luhr, B. Giannetti. **The brown leucitic tuff of Roccamonfina volcano (Roman Region, Italy).** Contrib. Mineral. Petrol., 95 (1987), pp. 420-436.

F. Masini, B. Sala. **Considerations on an integrated biochronological scale of italian Quaternary continentals mammals. Il Quaternario.** Ital. J. Quat. Sci., 24 (2011), pp. 193-198.

V. Michel, G. Shen, C.C. Shen, C.C. Wu, C. Verati, S. Gallet, M.H. Moncel, J. Combier, S. Khatib, M. Manetti. **Application of U/Th and $^{40}Ar/^{39}Ar$ dating to orgnac 3, a late Acheulean and early middle palaeolithic site in Ardeche, France.** PLoS One, 8 (12) (2013), p. e82394.

D. Moreno, C. Falguères, A. Pérez-González, P. Voinchet, B. Ghaleb, J. Despriée, J.J. Bahain, R. Sala, Carbonell, J.M. Bermúdez de Castro, J.L. Arsuaga. **New radiometric dates on the lowest stratigraphical section (TD1 to TD6) of Gran Dolina site (Atapuerca, Spain).** Quat. Geochronol., 30 (2015), pp. 535-540.

B. Muttillo, G. Lembo, C. Peretto. **L'insediamento a bifacciali di Guado San Nicola, Monteroduni, Molise, Italia.** Ann. dell'Università degli Studi Ferrara, 10/1 (2014), p. 166. Sez. Museologia Scientifica e Naturalistica

S. Nomade, P.R. Renne, N. Vogel, A.L. Deino, W.D. Sharp, T.A. Becker, A.R. Jaouni, R. Mundil. **Alder Creek sanidine (ACs-2), A Quaternary $^{40}Ar/^{39}Ar$ dating standard tied to the Cobb Mountain geomagnetic event.** Chem. Geol., 218 (2005), pp. 315-338.

S. Nomade, A. Gauthier, H. Guillou, J.F. Pastre. **$^{40}Ar/^{39}Ar$ temporal framework for the Alleret maar lacustrine sequence (French Massif Central): volcanological and Paleoclimatic implications.** Quat. Geochronol., 5 (2010), pp. 20-27.

A. Pereira, S. Nomade, P. Voinchet, J.J. Bahain, C. Falguères, H. Garon, D. Lefèvre, J.P. Raynal, V. Scao, M. Piperno. **The earliest securely dated hominin fossil in Italy and evidence of Acheulian occupation during glacial MIS 16 at Notarchirico (Venosa, Basilicata, Italy).** J. Quat. Sci. (2015), 10.1002/jqs.2809.

C. Peretto, M. Arzarello, J.J. Bahain, Boulbes, M. Coltorti, A.N. De Bonis, E. Douville, C. Falguères, N. Frank, T. Garcia, G. Lembo, Moigne, V.A.M. Morra, B. Muttillo, S. Nomade, Q. Shao, A. Perrotta, P. Pieruccini, M. Rufo, B. Sala, C. Scarpati, U. Thun Hohenstein, U. Tessari, M.C. Turrini, C. Vaccaro. **L'occupazione umana del Pleistocene medio di Guado San Nicola (Monteroduni, Molise).** Ann. dell'Università Ferrara, Museol. Sci. Nat., 10 (2014), pp. 23-31.

C. Peretto, J. Arnaud, J. Moggi-Cecchi, G. Manzi, S. Nomade, A. Pereira, C. Falguères, J.J. Bahain, D. Grimaud-Hervé, C. Berto, B. Sala, G. Lembo, B. Muttillo, G. Gallotti, U. Thun Hohenstein, C. Vaccaro, M. Coltorti, M. Arzarello. **A human deciduous tooth and new $^{40}Ar/^{39}Ar$ dating results from the Middle Pleistocene archaeological site of Isernia La Pineta, southern Italy.** PLoS One, 10 (10) (2015), p. e0140091, 10.1371/journal.pone.0140091.

C. Peretto, M. Arzarello, J.J. Bahain, N. Boulbes, J.M. Dolo, E. Douville, C. Falguères, N. Frank, T. Garcia, G. Lembo, A.M. Moigne, B. Muttillo, S. Nomade, A. Pereira, M.A. Rufo, B. Sala, Q. Shao, U. Thun Hohenstein, U. Tessari, M.C. Turrini, C. Vaccaro. **The Middle Pleistocene site of Guado San Nicola (Monteroduni, Central Italy) on the lower/middle palaeolithic transition.** Quat. Int. (2015), pp. 1-15, 10.1016/j.quaint.2015.11.056.

D. Phillips, E.L. Matchan. **Ultra-high precision $^{40}Ar/^{39}Ar$ ages for fish Canyon Tuff and Alder Creek Rhyolite sanidine: new dating standards required?** Geochim. Cosmochim. Acta, 121 (2013), pp. 229-239.

J.R. Prescott, J.T. Hutton. **Cosmic ray contributions to dose rates for luminescence and ESR dating: large depths and long-term time variations.** Radiat. Meas., 23 (1994), pp. 497-500.

P.R. Renne, A.L. Deino, W.E. Hames, M.T. Heizler, S.R. Hemming, K.V. Hodges, A.A.P. Koppers, D.F. Mark, L.E. Morgan, D. Phillips, B.S. Singer, B.D. Turrin, I.M. Villa, M. Villeneuve, J.R. Wijbrans. **Data reporting norms for 40Ar/39Ar geochronology.** Quat. Geochronol., 4 (2009), pp. 346-352.

P.R. Renne, R. Mundil, G. Balco, K. Min, K.R. Ludwig. **Response to the comment by W.H. Schwarz et al. on "Joint determination of ^{40}K decay constants and $^{40}Ar^*/^{40}K$ for the Fish Canyon sanidine standard, and improved accuracy for $^{40}Ar/^{39}Ar$ geochronology" by P.R. Renne et al. (2010).** Geochim. Cosmochim. Acta, 75 (2011), pp. 5097-5100.

T.A. Rivera, M. Storey, M.D. Schmitz, J.L. Crowley. **Age intercalibration of $^{40}Ar/^{39}Ar$ sanidine and chemically distinct U/Pb zircon populations from the Alder Creek Rhyolite Quaternary geochronology standard.** Chem. Geol., 345 (2013), pp. 87-98.

V. Rouchon, P.Y. Gillot, X. Quidelleur, S. Chiesa, B. Floris. **Temporal evolution of the Roccamonfina volcanic complex (Pleistocene), Central Italy).** J. Volcanol. Geotherm. Res., 177 (2008), pp. 500-514.

B. Sala, N. Boulbes, A.M. Moigne, U. Thun Hohenstein. **L'insieme faunistico del giacimento.** B. Muttillo, G. Lembo, C. Peretto (Eds.), L'insediamento a Bifacciali Di Guado San Nicola, Annali dell'Università degli Studi di Ferrara, Monteroduni, Molise, Italia (2014), pp. 59-78.

S. Scaillet, G. Vita-Scaillet, H. Guillou. **Oldest human footprints dated by Ar/Ar.** Earth Planet. Sci. Lett., 275 (2008), pp. 320-325

Q. Shao, J.J. Bahain, C. Falguères, C. Peretto, M. Arzarello, A. Minelli, U. Thun Hohenstein, J.M. Dolo, T. Garcia, N. Frank, E. Douville. **New ESR/U-series data for the early Middle Pleistocene site of Isernia la Pineta, Italy.** Radiat. Meas., 46 (2011), pp. 847-852.

Q. Shao, J.J. Bahain, C. Falguères, J.M. Dolo, T. Garcia. **A new U-uptake model for combined ESR/U-series dating of tooth enamel.** Quat. Geochronol., 10 (2012), pp. 406-411.

R.H. Steiger, E. Jäger. **Subcommission on geochronology: convention on the use of decay constants in geo- and cosmochronology.** Earth Planet. Sci. Lett., 6 (1977), pp. 359-362.

M. Terradillos-Bernal, J.C. Díez-Fernández-Lomana. **La transition entre les Modes 2 et 3 en Europe : le rapport sur les gisements du Plateau Nord (Péninsule Ibérique).** L'anthropologie, 16 (2012), pp. 348-363.

A. Tuffreau, A. Lamotte, E. Goval. **Les Industries acheuléennes de la France septentrionale.** L'Anthropologie, 112 (2008), pp. 104-139.

M.C. Turrini, G. Lembo, C. Peretto, U. Tessari, C. Vaccaro. **La serie stratigrafica.** B. Muttillo, G. Lembo, C. Peretto (Eds.), L'insediamento a Bifacciali Di Guado San Nicola, Annali dell'Università degli Studi di Ferrara, Monteroduni, Molise, Italia (2014), pp. 25-48.